Mechanical Behavior and Microhardness of Swollen Natural Rubber Loaded with Carbon Black

M. Abu-Abdeen, Abdalaziz A. Almulhem, A. Sedky*

Physics Department, Faculty of Science, King Faisal University, Al-Hassa 31982, P.O. Box 400, Kingdom of Saudi Arabia

Received 4 September 2007; accepted 8 March 2008
DOI 10.1002/app.28382
Published online 27 May 2008 in Wiley InterScience (www.interscience.wiley.com).

ABSTRACT: The mechanical behavior and microhardness characteristics of a natural rubber vulcanizate loaded with 40 phr high abrasion furnace carbon black swollen in kerosene were studied. The measured parameters (i.e., the Young's modulus, tensile strength, and elongation at break) varied with the swelling time in kerosene. The hardness degree decreased as the swelling time in kerosene increased. Different models were applied to describe this mechanical behavior. The Mooney–Rivilin relation agreed with the experimental data at low extension ratios, whereas the Blatz relation agreed at high extension ratios only. The strain rate sensitivity was taken into account to describe this mechanical behavior. The strain energy density as a function of the swelling time in kerosene was calculated with three different equations. © 2008 Wiley Periodicals, Inc. J Appl Polym Sci 109: 3361–3368, 2008

Key words: additives; blending; hardness; rubber; stress

INTRODUCTION

Polymeric materials have an enormous and intriguing range of desirable features. This is basically due to the linking and arrangement of their smaller units or monomers. The syntheses, arrangements, and conformations of these monomeric units result in a class of materials with a range of various properties.[1] The many attractive mechanical characteristics of polymers have made it desirable to choose these materials over traditional materials for numerous types of applications, such as binder constituents in explosives, load-bearing components, and jet engine modules. As the uses of polymers increase, an understanding of the mechanical behavior of these materials becomes vital for creating innovative and economical designs for various components. Polymers have more complicated properties as they display elastic and viscous responses at different strain rates and temperatures.[2,3]

Rubber elastomers are usually nonresistant to oils, greases, or fuels and therefore are swollen by them. This causes changes in their mechanical characteristics (particularly their moduli and loss angles) and shortens the time of exploitation.[4–8] There are a lot of publications concerning the influence of many factors on the mechanical and dynamic properties of rubbers.[9–13] However, only a few of them take into account the significance of the problem (practical and theoretical) of the influence of vulcanizates swollen by liquids on their mechanical properties.

Models of deformation in polymers have been investigated for a long time. The classical kinetic theory[14–16] attributed the high elasticity of a cross-linked rubber to the change in the conformational entropy of the long, flexible molecular chains. A nonlinear viscoelastic constitutive model based on the assumptions of nonlinear elasticity and linear viscoelasticity has been developed.[17] The basic formulation assumes stress relaxation functions with two different relaxation times to describe strain rate effects. The strain energy functions have been commonly used to describe the mechanical properties of rubber or rubberlike materials under quasistatic loading conditions. Using a strain energy function and a stress relaxation function with only one relaxation time, a viscohyperelastic model that combines static hyperelastic behavior and a viscoelastic model for incompressible-like rubber materials has been presented.[18] Reese[19] developed a material model for the thermoviscoelastic behavior of rubberlike polymers that is based on transient network theory. There are also some other studies dealing with polymer modeling based on overstress[20–22] and shape-memory polymers.[23]

On the other hand, the measurement of the hardness degree may be important for assessing product performance and is used in the identification,

Correspondence to: M. Abu-Abdeen, Physics Department, Faculty of Science, Cairo University, Giza, Egypt (mmaabdeen@yahoo.com).
**Permanent address:* Physics Department, Faculty of Science, Assiut University, Assiut, Egypt.

© 2008 Wiley Periodicals, Inc.

TABLE I
Recipe of the 40HAF/NR Composites

	Ingredient							
	NR	HAF	Processing oil	Stearic acid	MBTS[a]	PBN[b]	Zinc oxide	Sulfur
phr	100	40	10	2	2	1	5	2

[a] Dibenthiazole disulfate.
[b] Phenyl-β-naphthylamine.

classifications, and quality control of products. Hardness tests provide a rapid evaluation of variations in mechanical properties affected by changes in the chemical or processing conditions, the addition of compounding ingredients, heat treatments, swelling, aging, and the microstructure of the samples. Microhardness measurement offers a nondestructive technique for studying the mechanical behavior of materials, and it is applied to polymeric materials widely now.[24–27]

The interaction of polymeric materials with different solvents is an important problem from both academic and technological points of view.[28–30] Crosslinked polymers brought into contact with different solvents during service applications usually exhibit the phenomenon known as swelling. The capacity of crosslinked polymers for the degree or amount of swelling assesses swelling expressed as the amount of liquid absorbed by the polymer. The swelling properties of polymers are mainly related to the elasticity of the network, the extent of crosslinking, and the porosity of the polymer.[31,32] The determination of the resistance of a polymer to solvents and gases is standardized in test procedures before the polymer finds successful applications involving exposure to such solvents and gases.[33,34]

The objective of this work was to study the effect of swelling in kerosene on both uniaxial stress–strain behavior under tension and the hardness degree of natural rubber (NR) vulcanizates loaded with 40 phr high abrasion furnace (HAF) carbon black. We also sought to develop a simple and flexible phenomenological constitutive model to characterize the observed dependence of the mechanical behavior on the time of swelling in kerosene.

EXPERIMENTAL

Compounding and curing

A master batch of NR loaded with 40 phr HAF carbon black (N-330) was prepared. Samples were prepared according to the recipe presented in Table I. The compounds were mixed according to ASTM D 3182 in a laboratory-sized mixing mill at a friction ratio of 1:1.19 by careful control of the temperature, nip gap, time of mixing, and uniform cutting operation. The temperature range for mixing was 60–70°C. The order and time periods of mixing were as follows: 0–3 min of mastication, 3–6 min of adding one-third of the filler plus one-third of the processing oil, 6–13 min of adding one-third of the filler and one-third of the oil, 13–18 min of adding the remaining filler and oil, 18–26 min of adding other ingredients, and 26–30 min of refining through a tight nip gap and dump (the nip gap was 1.5 mm). After mixing, the rubber compositions were molded in an electrically heated hydraulic press to the optimum cure with molding conditions that were previously determined from torque data with a Monsanto R100 rheometer (New York).

Testing

The tensile tests were determined on unswollen and swollen dumbbell-shaped specimens. The measurements were carried out at 25°C on an Instron 3345J8621 (Norwood) tensile machine with a grip separation of 40 mm at a crosshead speed of 500 mm/min per ASTM D 412 and ASTM D 624, respectively.

The hardness (Shore A) of the studied samples was determined with a Zwick/Roell 3130/3131 DGM 93 18 389.5 hardness tester (Ulm, Germany) in accordance with ASTM D 2240-05. The tests were performed on unswollen and swollen samples 30 mm in diameter and 6 mm thick. The readings were taken after 10 s of indentation after firm contact had been established with the specimen.

RESULTS AND DISCUSSION

Stress–strain curves

The stress–strain curves of 40HAF/NR vulcanizates at different swelling times in kerosene are shown in Figure 1. At strains lower than 20%, the kinetic theory holds. At large deformations, there is limited extensibility of the crosslinked chains. Meanwhile, there is a stress-softening effect at moderate strains. Separate plots (not shown here) of $d\sigma$ (Stress)/$d\varepsilon$ (Strain) versus ε were determined for all swelling times. They showed strain-independent regions at very low strain values. These constant values are taken to be Young's modulus (E) at different swelling times, which are shown in Figure 2. A sharp decrease in the values of E can be observed at low

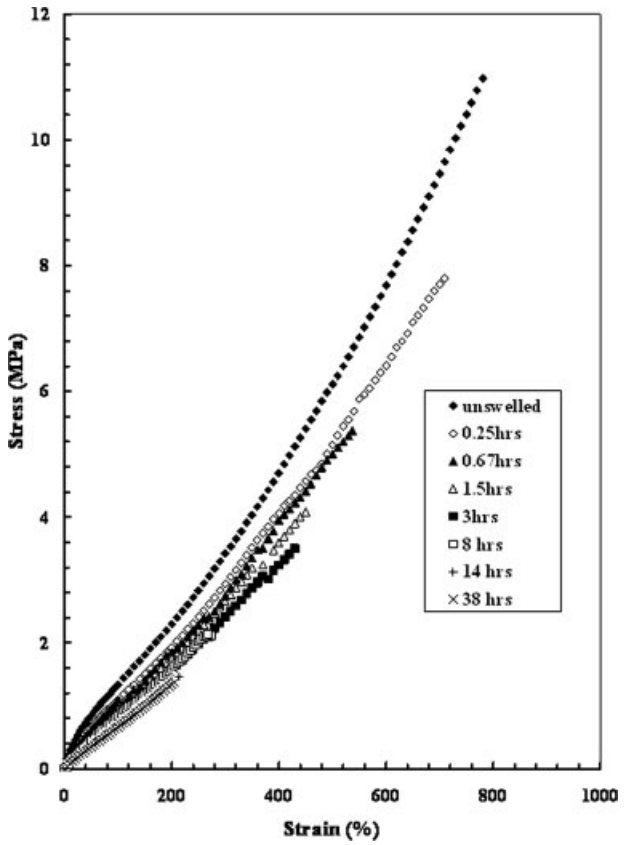

Figure 1 Stress–strain curves for 40HAF/NR vulcanizates with different immersion times in kerosene.

swelling times up to approximately 3 h, and this is followed by a gradual decrease up to 40 h. The reduction of E could be due to plasticization by the absorbed kerosene and the disruption of hydrogen bonds between the molecular chains in the rubber matrix.

The effect of the swelling time in kerosene on the tensile strength (σ_b) for NR vulcanizates loaded with 40 phr HAF is shown in Figure 3. σ_b for the vulcanizates decreases sharply with the time of swelling increasing up to 3 h, and it seems to be time-independent after approximately 10 h. The same behavior has been recorded for the elongation at break (ε_b), as shown in Figure 4.

Both σ_b and ε_b obey an empirical formula of the following form:

$$F(t) = F_0[A\exp(-at) + B\exp(-bt)] \quad (1)$$

where $F(t)$ describes either σ_b or ε_b and F_0 is the tensile strength for unswollen samples (10.88 MPa) when $F(t)$ is the tensile strength or the elongation at break for the same samples (782%) when $F(t)$ is the elongation at break. A, B, a (i.e., $1/\tau_1$) and b (i.e., $1/\tau_2$) are constants, and their values were estimated with the iterative method and are shown in Table II.

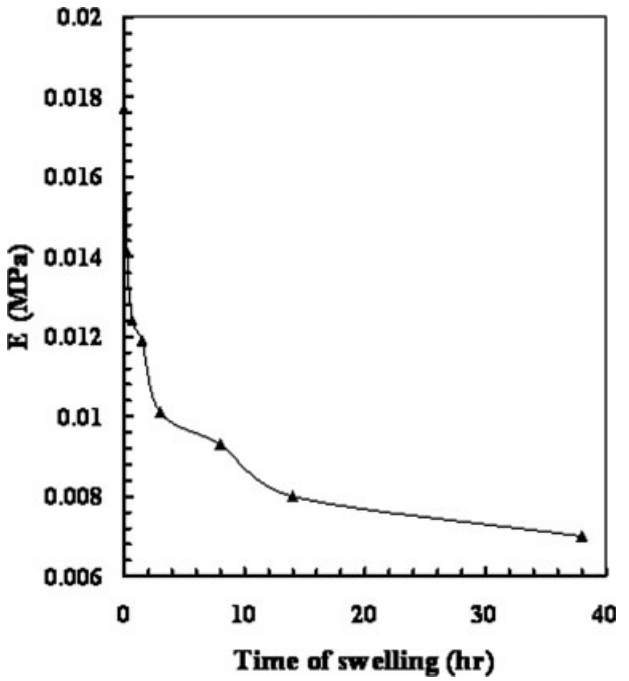

Figure 2 Dependence of E of 40HAF/NR vulcanizates on the time of swelling in kerosene.

The constants τ_1 and τ_2 are considered the relaxation times needed for rubber chains to take a new configuration under the effect of swelling with short and long swelling times, respectively. This is because the values of τ_1 [which affects the behavior of $F(t)$ for short times of swelling] are low compared with those of τ_2 [which affects the behavior of $F(t)$ for relatively long times of swelling]. The values of τ_1 may

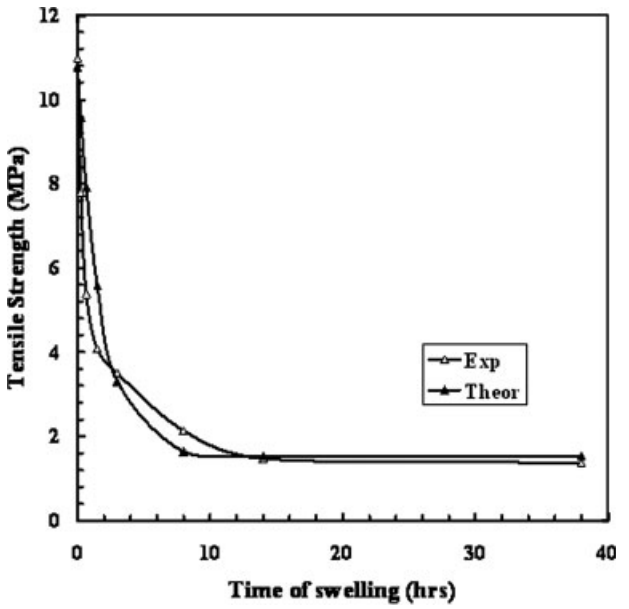

Figure 3 Dependence of σ_b of 40HAF/NR vulcanizates on the time of swelling in kerosene.

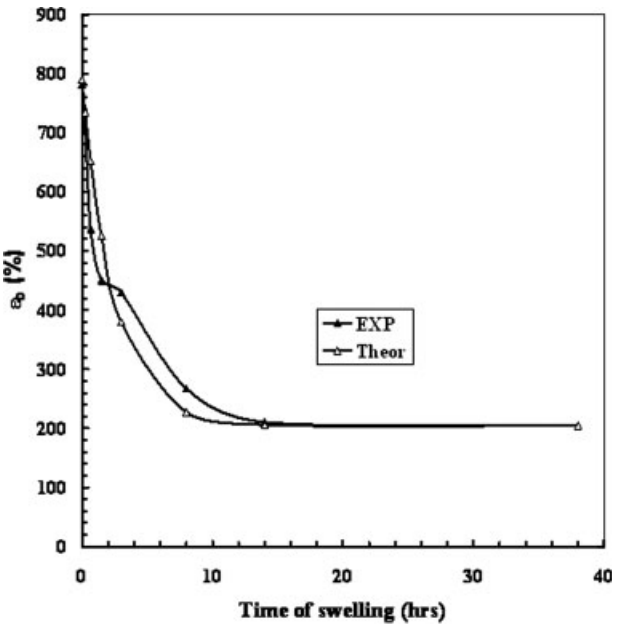

Figure 4 Dependence of ε_b of 40HAF/NR vulcanizates on the time of swelling in kerosene.

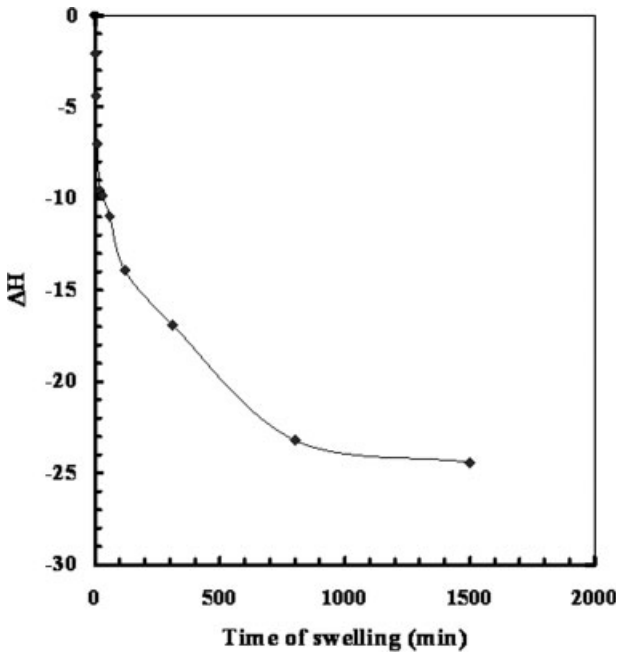

Figure 5 Dependence of the difference in the hardness degree (ΔH) of 40HAF/NR vulcanizates on the time of swelling in kerosene.

indicate that the rubber chains take a short time to return to their original configuration when swollen for short intervals of time in kerosene, and this time becomes longer when a sample is swollen for long times, as indicated by the values of τ_2.

Microhardness

Figure 5 illustrates the dependence of the difference in the hardness degree with the swelling time. It shows an abrupt decrease at short swelling times followed by a slow decrease at long swelling times in accordance with E. The degree of hardness (H) is related to E according to the following relation:[6]

$$E_s/E_0 = mH/(100 - mH) \quad (2)$$

where E_s and E_0 are the tensile elastic moduli for the swollen and unswollen samples, respectively, and m is a conversion factor, the value of which is determined with $E_s/E_0 = 1$ and $H = 66.86$ for an unswollen sample. The value of m was found to equal 0.748. Figure 6 shows the variation of E_s/E_0 and H_s/H_0 (where H_s and H_0 are the hardness degrees of swollen and unswollen samples, respectively) with the swelling time in kerosene. A good agreement between the values from eq. (2) and the experimental values of E displayed previously in Figure 2 can be observed in Figure 6. The decrease in either E or H may be attributed to the weakness or degradation of the rubber–filler and filler–filler interactions and/or the predominance of chain scissions and reversion.

TABLE II
Calculated Values of Constants *A*, *B*, *a*, and *b*

	Physical property			
	A	B	$\tau_1 = 1/a$ (h)	$\tau_2 = 1/b$ (h)
For σ_b	0.85	0.14	1.82	1.00×10^4
For ε_b	0.75	0.26	2.5	6.67×10^3

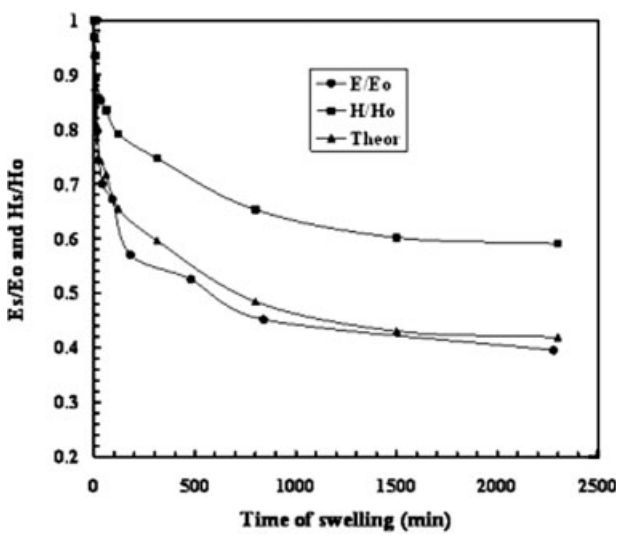

Figure 6 Dependence of both E_s/E_0 and H_s/H_0 of 40HAF/NR vulcanizates on the time of swelling in kerosene.

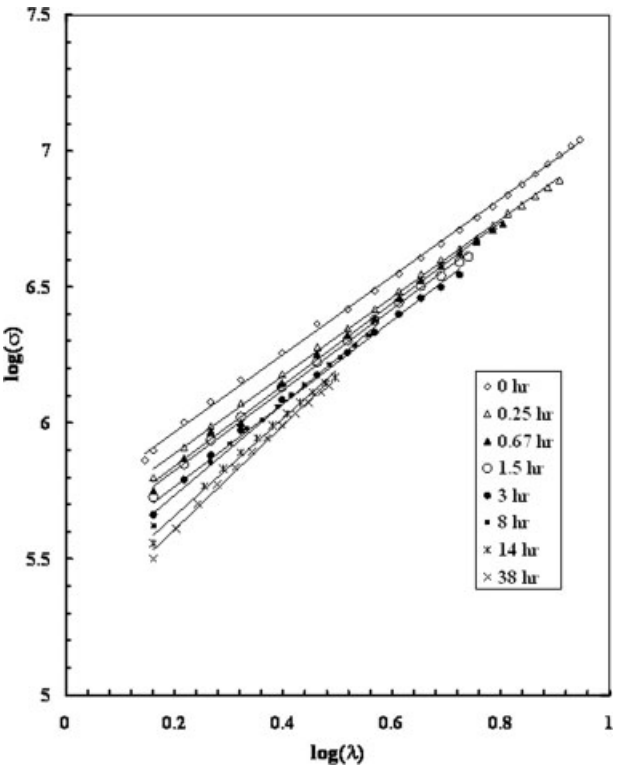

Figure 7 Dependence of log σ on log λ of 40HAF/NR vulcanizates with different times of swelling in kerosene.

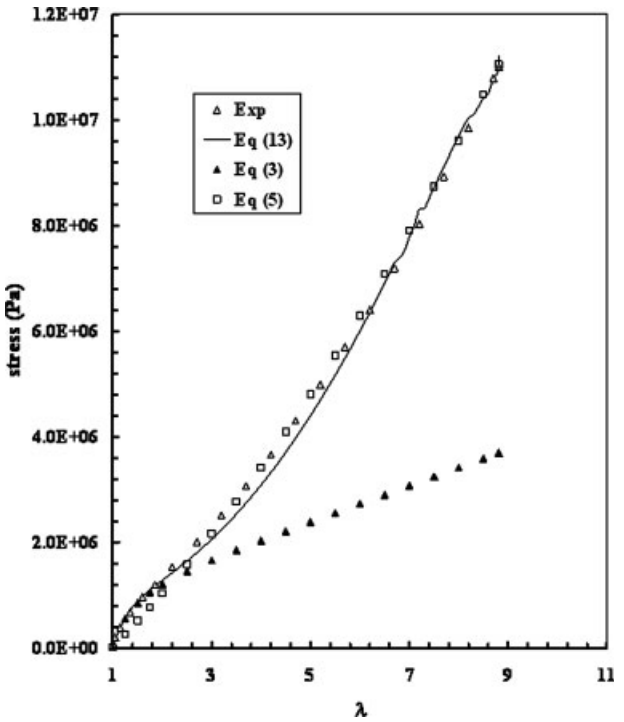

Figure 8 Dependence of σ on λ of unswollen 40HAF/NR vulcanizates.

Theoretical models

It has been reported[35] that the stress–strain behavior of rubber vulcanizates can be described by the Mooney–Rivilin (MR)[36] relation, which in a simple extension gives

$$\frac{\sigma}{2(\lambda - \lambda^{-2})} = C_1 + C_2\lambda^{-1} \quad (3)$$

where σ is the true stress, which produces extension ratio λ in the sample, and C_1 and C_2 are parameters characteristic of the rubber vulcanizate whose values are readily determined from σ–λ plots, as shown later in Figures 8–12. These values are tabulated in Table III. The constant C_1 describes the behavior predicted by the statistical theory of rubberlike elasticity, and its value is directly proportional to the number of network chains per unit of volume of the rubber.[37] The value of C_2 determines the number of steric obstructions and the number of effectively trapped elastic entanglements as well as other network defects.[38] In the case of a long time of immersion for vulcanizates in kerosene, effects such as the degradation and isolation of network crosslinks result in a reduction of the number of networks, and a reduction of steric obstructions and other network defects becomes possible. These effects are manifested as decreases in the values of C_1 and C_2 with swelling in kerosene. On plotting σ versus λ, as shown later in Figures 8–12 for different immersion times of the studied samples in kerosene, one can obtain an agreement between the experimental values and MR relation at low λ values, whereas a deviation between them appears at moderate strains, and it becomes highest at high strains.

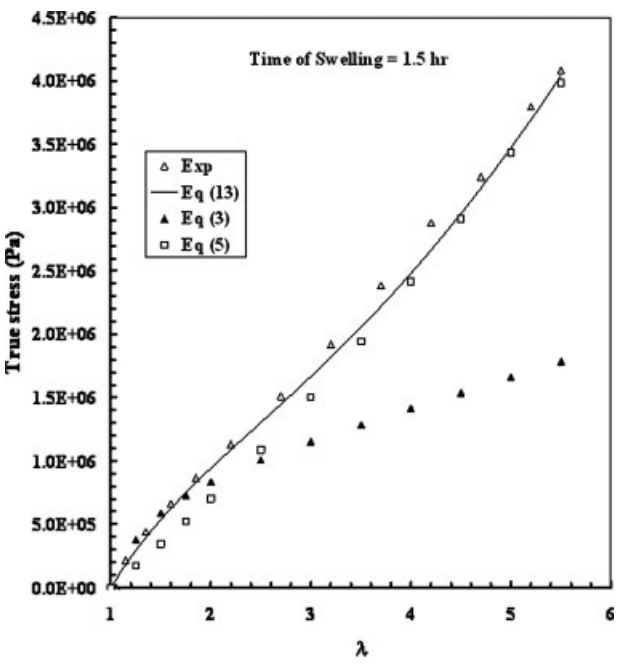

Figure 9 Dependence of σ on λ of 40HAF/NR vulcanizates when swollen in kerosene for 1.5 h.

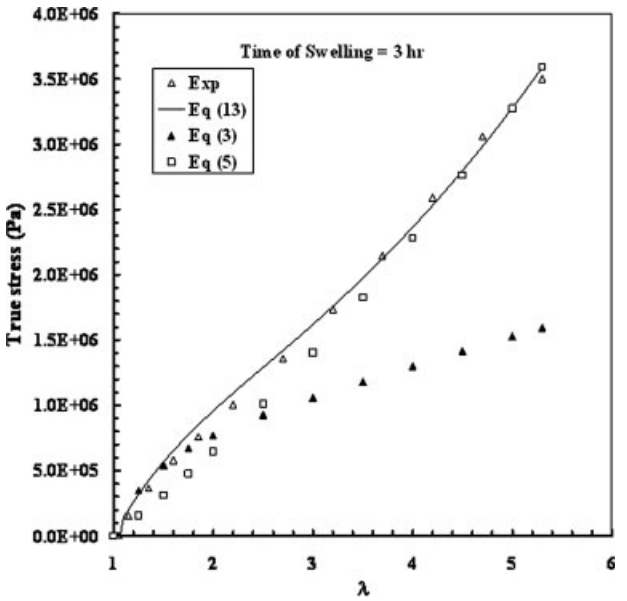

Figure 10 Dependence of σ on λ of 40HAF/NR vulcanizates when swollen in kerosene for 3 h.

The strain energy density (W) associated with this deformation is determined as follows:[39]

$$W = -1/2kT\nu[\lambda^2 + (2/\lambda) - 3] \quad (4)$$

where k is Boltzmann's constant, ν is the number of effective plastic chains per unit of volume, and T is the absolute temperature. The values of ν are calculated from the slopes of separate plots (not mentioned here) between σ and $(\lambda^2 - \lambda^{-1})$.[40]

Blatz et al.[41] showed that it is possible to represent the stress–strain behavior of several rubberlike materials by a very simple stress–strain relation in which the strain is based on the n measure, with n being adjusted to fit the appropriate material data. According to Blatz et al., the true stress–strain extension ratio [σ(λ)], under simple tension conditions, is given by a simple form, in which the strain is based on the n measure considered by Sethe[42] as follows:

$$\sigma(\lambda) = 2(G/n)(\lambda^n - \lambda^{-n/2}) \quad (5)$$

where G is the shear modulus. In this equation, σ(λ) is derived from the strain energy density equation [$w(\lambda)$]:

$$w(\lambda) = 2(G/n^2)(\lambda^n + 2\lambda^{-n/2} - 3) \quad (6)$$

n is independent of temperature and is considered to be a material constant as well as a kinematic quantity for unswollen rubber vulcanizates. More-

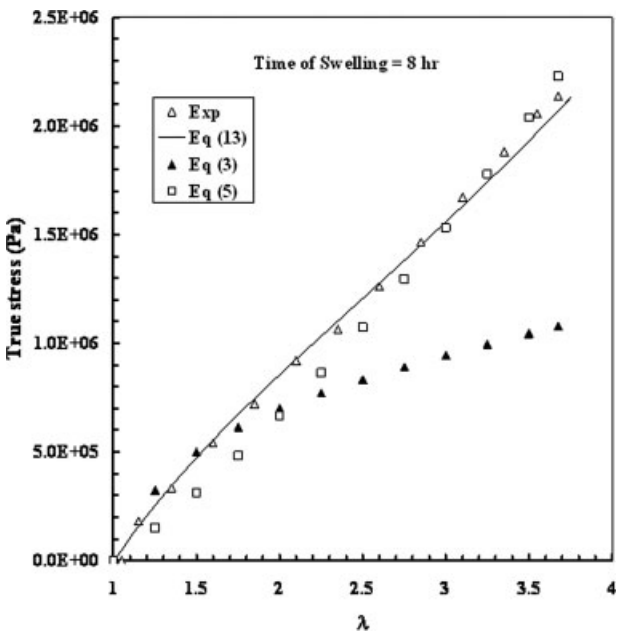

Figure 11 Dependence of σ on λ of 40HAF/NR vulcanizates when swollen in kerosene for 8 h.

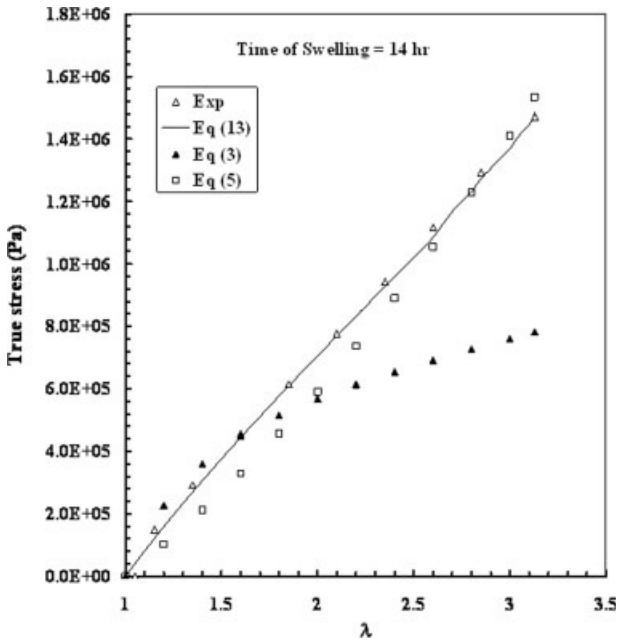

Figure 12 Dependence of σ on λ of 40HAF/NR vulcanizates when swollen in kerosene for 14 h.

TABLE III
Calculated Values of the Constants in Eqs. (3), (5), (7), and (13)

t (h)	C_1 (MPa)	C_2 (MPa)	D_0 (MPa)	G (MPa)	E_0 (MPa)	n	ε_r
0	0.170	0.350	0.145	0.355	0.453	1.43	0.30
0.25	0.145	0.290	0.120	0.290	0.380	1.44	0.50
0.67	0.130	0.249	0.113	0.250	0.347	1.50	0.60
1.5	0.120	0.238	0.108	0.240	0.334	1.49	0.82
3	0.110	0.220	0.100	0.220	0.294	1.53	0.70
8	0.090	0.220	0.100	0.220	0.280	1.69	1.00
14	0.070	0.185	0.084	0.190	0.237	1.80	1.38
38	0.066	0.170	0.077	0.170	0.214	1.92	1.45

over, El-Lawindy and El-Guiziri[43] found that the n measure is still a material constant, even after the addition of carbon black, but with higher values than those for unloaded rubber.

The stress–strain value [eq. (5)] was approximated by Malkin et al.[44] as follows:

$$\log\left(\frac{2\sigma}{3E_0}\right) = n\log\lambda - \log n \tag{7}$$

where E_0 is a constant. A suggested graphical method for determining the constants n and E_0 by the construction of a plot of log σ versus log λ is shown in Figure 7. The n measure is obtained from the slopes, whereas E_0 is obtained from the intercept of the fitted curves. These values are listed in Table III, and it can be observed that E_0 decreases with increasing swelling time in kerosene as a result of the cession of rubber chains due to internal pressure caused by solvent molecules. The kerosene molecules occupy positions between the rubber molecules, forcing these macromolecules apart and producing internal strains.

These calculated values of both E_0 and n were used in eq. (5). Then, a plot of σ(λ) versus λ was constructed for the studied vulcanizates at different swelling times in kerosene, as shown in Figures 8–12, and the values of G were calculated. A fairly good agreement between experimental and theoretical values was obtained at high strains, and a small deviation between them took place at low strain values.

From this discussion, we can observe that the MR relation fits the experimental values well at low strains, whereas the Blatz equation agrees at high strains; however, it does not satisfy the E/G relation. To achieve a full description of the uniaxial stress–strain behavior of a rubber matrix, it was determined to be strain-rate-sensitive and nonlinear.[45,46] The stress can be represented as follows:

$$\sigma = f(\varepsilon)g(\dot{\varepsilon}) \tag{8}$$

where $f(\varepsilon)$ represents the strain-rate-independent behavior and $g(\dot{\varepsilon})$ accounts for the effects of the strain rate. With these considerations, Song et al.[47] derived the strain-rate-dependent constitutive model for rubber, which is represented as follows:

$$\sigma = D_0(\lambda^2 - \lambda^{-1}) + g_1(\dot{\varepsilon})(\lambda - \lambda^{-2}) + g_2(\dot{\varepsilon})\left[1 - \exp\left(\frac{\lambda - 1}{\varepsilon_r}\right)\right] \tag{9}$$

where D_0 and ε_r are constants and $g_1(\dot{\varepsilon})$ and $g_2(\dot{\varepsilon})$ correspond to strain rate effects at large and small strains, respectively. Formulations have recently been used to describe the strain rate effects of materials containing metals[48] and composites[49] in the following form:

$$g(\dot{\varepsilon}) = a' + b'(\dot{\varepsilon})^{\alpha} \tag{10a}$$

or

$$g(\dot{\varepsilon}) = a' + b_1\left(\frac{\dot{\varepsilon}}{\dot{\varepsilon}_0}\right)^{\alpha} \tag{10b}$$

where $\dot{\varepsilon}$ is the reference strain rate; $\dot{\varepsilon}_0$, α, a', and b' are material constants; and $b_1 = b'\dot{\varepsilon}_0^{\alpha}$. The strain-rate-dependent model for rubber can be expressed as follows:

$$\sigma = D_0(\lambda^2 - \lambda^{-1}) + \left[A_0 + A_1\left(\frac{\dot{\varepsilon}}{\dot{\varepsilon}_0}\right)^{\alpha}\right][\lambda - \lambda^{-2}] + \left[B_0 + B_1\left(\frac{\dot{\varepsilon}}{\dot{\varepsilon}_0}\right)\right]\left[1 - \exp\left(-\frac{\lambda - 1}{\varepsilon_r}\right)\right] \tag{11}$$

where A_0, A_1, B_0, and B_1 are constants. The strain energy density (W) takes the following form:

$$W = 1/2D_0\left(\lambda^2 + \frac{2}{\lambda} - 3\right) + B_1\left(\frac{\dot{\varepsilon}}{\dot{\varepsilon}_0}\right)\left(\frac{1}{\lambda^2} + 2\lambda - 3\right) \tag{12}$$

The stress–strain behavior of the studied samples was checked with eq. (11), and a fairly good agreement was observed between them, as shown in Figures 8–12. Interestingly, the second term in eq. (11), $[A_0 + A_1\left(\frac{\dot{\varepsilon}}{\dot{\varepsilon}_0}\right)^{\alpha}](\lambda - \lambda^{-2})$, has no significant effect on the behavior of the studied samples. Moreover, when this term is deleted from the equation, the behavior is unchanged. Therefore, eq. (11) could be written as follows:

$$\sigma = D_0(\lambda^2 - \lambda^{-1}) + \left[B_0 + B_1\left(\frac{\dot{\varepsilon}}{\dot{\varepsilon}_0}\right)\right]\left[1 - \exp\left(-\frac{\lambda - 1}{\varepsilon_r}\right)\right] \tag{13}$$

The parameters B_0, B_1, and $\dot{\varepsilon}_0$ have constant values of 0.8 MPa, $-$ 6.3 $\times$ 10^{-6} MPa, and 0.004, respectively, and are independent of the time of swelling in kerosene. The values of D_0 and ε_r are listed in Table III. First, $G \approx C_2$, so one can describe G with the constant C_2 in the MR equation, and second, $D_0 \approx \frac{1}{2}C_2 \approx \frac{1}{2}G$.

The dependence of the calculated strain energy density on the time of swelling in kerosene for the investigated composites for the three different models discussed previously in this work is shown in Figure 13 at an elongation ratio of 2. This energy density is calculated with eqs. (4), (6), and (12). It always decreases with the time of swelling increasing for the three discussed models. This indicates that at small intervals of rubber immersion in kerosene, all the chains need energy to be deformed. As the time of swelling is increased, the number of chains that need energy for deformation becomes less,

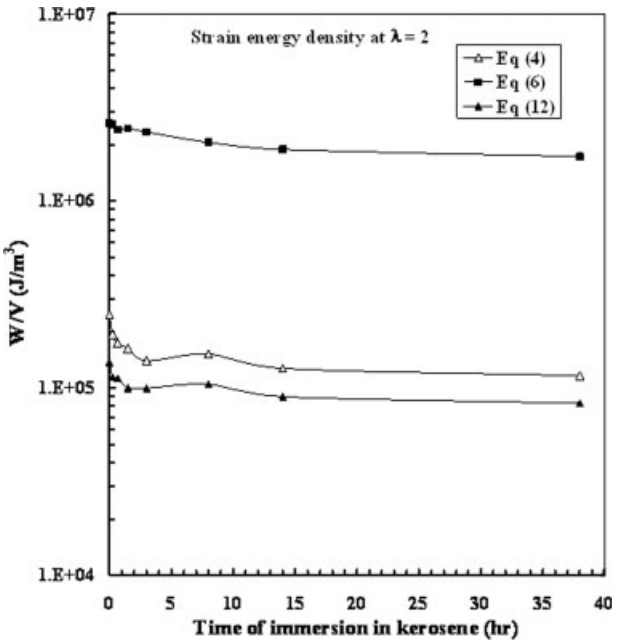

Figure 13 Dependence of the strain energy density (W/V) on the swelling time of 40HAF/NR at $\lambda = 2$.

and this results in a small change in the energy density, which appears time-independent, as shown in Figure 13. In addition, there is an approximate coincidence between the values of the strain energy density calculated with eqs. (4) and (12) at this value of λ. On the other hand, these values are far from those calculated with eq. (6), and this may be referred to the agreement between the classical theory and the strain rate considerations at low strains.

CONCLUSIONS

From this study, it is concluded that the swelling of NR vulcanizates loaded with HAF carbon black in kerosene reduces E, σ_b, ε_b, H, and W. The MR model agrees with the experimental data at low strains, whereas the Blatz model agrees at high strains. The strain rate sensitivity is embedded to describe the strain rate dependence at both large and small strains. The model exhibits good agreement with the experimental results over a wide range of strains. The relatively small number of material constants and simple formulation increase the applicability of the model in numerical analysis. G can be determined from the constant C_2 in the MR relation.

The authors acknowledge the Deanship of Scientific Research and Faculty of Science, King Faisal University, for providing the facilities required for this investigation.

References

1. Painter, P. C.; Coleman, M. M. Fundamentals of Polymer Science: An Introductory Text, 2nd ed.; Technomic: Lancaster, PA, 1997.
2. Haupt, P.; Lion, A.; Backhaus, E. Int J Solids Struct 2000, 37, 3633.
3. Ehlers, W.; Markert, B. Int J Plast 2003, 19, 961.
4. Gajewski, M. Polimery-Tworzywa Wielkoczasteczkowe 1974, 19, 244.
5. Busfield, J. J. C.; Deeprasertkul, C.; Thomas, A. G. Polymer 2000, 41, 9219.
6. Rzymski, W. M.; Jentzsch, J. Plast Kautsch 1990, 37, 48.
7. Shaefer, R. J Rubber World 1995, 222, 16.
8. Magryta, J.; De Bek, C.; De Bek, D. J Appl Polym Sci 2006, 99, 2010.
9. Dannenberg, E. M. Rubber Chem Technol 1975, 48, 410.
10. Wang, M. J. Rubber Chem Technol 1998, 71, 520.
11. Medalia, A. I. Rubber Chem Technol 1978, 51, 437.
12. Payne, A. R. J Polym Sci 1962, 6, 57.
13. Magryta, J. Eur Polym J 1991, 27, 359.
14. Wall, F. T. J Chem Phys 1943, 11, 527.
15. Flory, P. J. Polymer Chemistry; Cornell University Press: Ithaca, NY, 1953.
16. James, H. M.; Guth, E. J Chem Phys 1943, 11, 455.
17. Wang, L. L.; Huang, D.; Gan, S. In Constitutive Relations in High/Very High Strain Rates; Kawata, K.; Shioiri, J., Eds.; IUTAM Symposium: Noda, Japan, 1995; p 137.
18. Yang, L. M.; Shim, V. P. W.; Lim, C. T. Int J Impact Eng 2000, 24, 545.
19. Reese, S. Int J Plast 2003, 19, 909.
20. Krempl, E.; Khan, F. Int J Plast 2003, 19, 1069.
21. Colak, O. Int J Plast 2005, 21, 145.
22. Akhtar, S. K.; Oscar, L. P.; Rehan, K. Int J Plast 2006, 22, 581.
23. Liu, Y.; Gall, K.; Dunn, M. L.; Greenberg, A. R.; Diani, J. Int J Plast 2006, 22, 279.
24. Tangorra, G. Rubber Chem Technol 1966, 39, 1520.
25. Stiehler, R. D.; Decker, G. E.; Bullnau, G. W. Rubber Chem Technol 1975, 48, 255.
26. Waters, N. E. J Appl Phys 1965, 16, 577.
27. Gonzalez, A.; Martin-Gil, J.; De Saja, J. A. J Appl Polym Sci 1986, 31, 717.
28. Barton, J. O. Polymer 1979, 20, 1018.
29. Ito, K. J Polym Sci Polym Chem Ed 1978, 16, 497.
30. Ateia, E. J Appl Polym Sci 2005, 95, 916.
31. Hashim, A. S.; Ong, S. K. Polym Int 2002, 51, 611.
32. Sobhy, M. S.; Mohdy, M. M. M.; Abdel-Bary, E. M. Polym Test 1997, 16, 349.
33. Mateo, J. L.; Bosch, P.; Senano, J.; Calvo, M. Eur Polym J 2000, 36, 1803.
34. George, S. C.; Knorgen, M.; Thomas, S. J Membr Sci 1999, 163, 1.
35. Mullins, L.; Tobin, N. R. J Appl Polym Sci 1965, 9, 2993.
36. Rivilin, R. S.; Sanders, D. W. Philos Trans R Soc A 1951, 213, 251.
37. Kontou, E.; Spathis, G. J Appl Polym Sci 1990, 39, 649.
38. Priss, L. S. J Polym Sci 1975, 3, 195.
39. Kumar, A.; Gupta, R. K. Fundamentals of Polymers; McGraw-Hill: New York, 1998; p 322.
40. Abu-Abdeen, M. J Appl Polym Sci 2001, 81, 2265.
41. Blatz, P. J.; Sharda, S. C.; Tschoegl, N. W. Trans Soc Rheol 1974, 18, 145.
42. (a) Sethe, B. R. In Second Order Effects in Elasticity, Plasticity and Fluid Mechanics; Reiner, M.; Abir, D., Eds.; McMillan: New York, 1964; p 162;. (b) Sethe, B. R. Proc Int Cong Appl Mech 1964, 11, 383.
43. El-Lawindy, A. M.; El-Guiziri, S. B. J Phys D 2000, 33, 1.
44. Malkin, Y. A.; Sabasi, Y. U.; Beghishev, V. P. Int J Polym Mater 1981, 9, 1.
45. Song, B.; Chen, W. J Eng Mater T ASME 2003, 40, 4719.
46. Cheng, M.; Chen, W. Int J Solids Struct 2003, 40, 4749.
47. Song, B.; Chen, W.; Cheng, M. J Appl Polym Sci 2004, 92, 1553.
48. Warren, T. L.; Forrestal, M. J. Int J Solids Struct 1998, 35, 3737.
49. Song, B.; Chen, W.; Weerasooriya, T. J Compos Mater 2003, 37, 1723.